MINIMIZING ARTIFICIAL STIFFNESS IN LINEAR TETRAHEDRAL ELEMENT USING VIRTUAL MESH REFINEMENT

S. Waluyo

Department of Industrial Engineering
University of Jenderal Soedirman
Purbalingga, Indonesia

ABSTRACT

This work presents a new method to minimize artificial stiffness in linear tetrahedral element using virtual mesh refinement (VRM) method. The basic idea behind this work is to give additional degree of freedom by using internal mesh over the linear tetrahedral element. This local internal mesh and its corresponding equilibrium condition under particular boundary condition are invisible to users or virtual. Using specialized displacement test vectors, strain energy is obtained and used to calculate reduction factor for artificial stiffness. Numerical experiments are performed at the end to briefly qualitatively show performance of our proposed method.

Keywords: Linear tetrahedral element, VMR, Strain energy, Displacement test vector.

1. INTRODUCTION

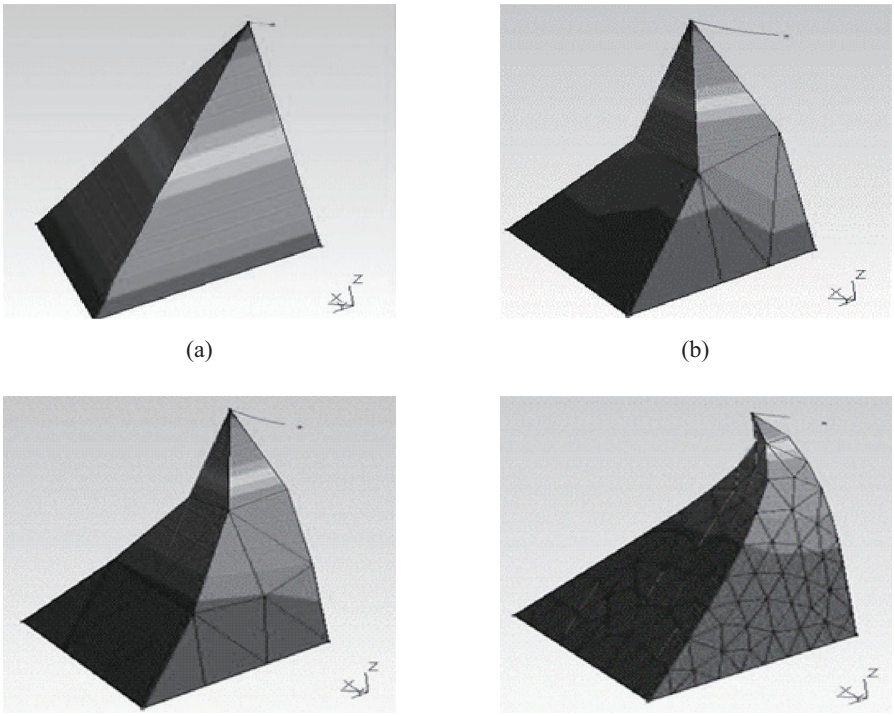
Linear 4-nodes tetrahedral finite element (FE) has been widely used for direct auto meshing for discretization of complex geometries. This type of element has been formulated at early development of finite element method for solid continua [1]. Programming task for this type element is relatively easier compared to other type of solid element since linear shape function is used. Recently, this element is considerably important to help complex microstructural design of advance material incorporating homogenization procedures, e.g. see [2]. However, this element has severe well-known drawback to have natural constant stress inside element due to application of linear shape function. In some case, e.g. close to stress concentration area, very dense meshing is required to achieve proper stress distribution. However, using very large number of element can increase engineering design time due to increasing of computational time.

To still work with optimum number of the element, some improvements have been proposed. The most straightforward solution are using mid-side nodes and quadratic shape function called quadratic tetrahedral element. Although this can reduce number of element used, the additional mid-side nodes still gives extra degree of freedom. On the other hand, transformation from parametric to global coordinate is not straightforward as linear element since it contains nonlinear equation. Meanwhile, by still relying on the 4-nodes a technique called mixed enhanced which use enhanced strain distribution is proposed by [3]. Alternatively, by maintaining linear function and implementing the Hu-Washizu principle Thoutireddy *et al.* in [4] develop a composite tetrahedral element with 10 nodes called "CT3D" by 12 ensemble of 4-nodes tetrahedral elements. Some recent articles regarding the improvement are relied on the popular smoothed method proposed by [5] and similar method as [4] but with improvement in integration scheme [6]. Although those aforementioned methods as well as other similar approaches work very well, they have been developed mainly using mathematical abstraction with less geometrical interpretation.

In this work, we revisit another alternative method proposed in [7] which relies on tetrahedral element ensemble as [4] but still using 4-nodes element namely the virtual meshing refinement (VMR). Instead of focusing on the potential implementation for finite strain problems as given in [7], we focus here only with small strain assumption but more detail in theoretical aspects. The basic idea is the same as [7] to give internal elements inside the original linear element as additional degree of freedom (DOF) instead of using continuous function. To keep visualization user-friendly, the internal elements and their nodes are not shown or virtual with respect to users. In this work, both original linear element, i.e. 4-nodes without additional DOF, and the internal element use small strain kinematics formulation. To account for minimizing artificial stiffness, strain energy from the original elements and modified element with the VMR method are compared to obtain strain energy ratio which is used to modify stiffness of the original linear element.

* Corresponding author (sugeng.waluyo@unsoed.ac.id)

DOI : 10.1017/jmech.2016.113
Copyright © 2016 The Society of Theoretical and Applied Mechanics
https://doi.org/10.1017/jmech.2016.113 Published online by Cambridge University Press



(a) (b)

(c) (d)

Fig. 1 FEM simulation of tetrahedron volume with different number of the internal elements from (a) single element to (d) 533 elements.

To compute strain energy, a specialized displacement vector is generated which depend on scalar measurement of tetrahedral shape quality called metric.

The advantage of using this proposed method is that we do not need complex mathematical formality to reduce the artificial stiffness in the linear tetrahedral element as the predecessor. What we need only geometrical interpretation with simple numerical algorithm to do the task and avoid to use many mathematical formalities in a variational problem to find appropriate functions as the additional degree of freedom. Beside that advantage, the main limitation of the proposed method is how to find better approximation for the energy ratio such that we can approximate the corresponding analytical solution of the problem if it exists.

We split this paper into four sections. This section gives overview why the proposed method is novel. In the next section, the underlying idea for the method is presented with detail theoretical aspects. Then, some numerical experiments from simple one element to more complex problems are presented and studied in the Third Section. Finally, at the last section we summarize some important remarks about the proposed method.

2. METHOD

2.1 Virtual Elements: Structure, Coordinate Transformation and Stiffness Matrix

In this section, two main important aspects to successfully implement the VMR method are presented, i.e. structure of the internal virtual elements and related coordinate transformation. First, for simplicity the shape of internal element used are also tetrahedral with 4-nodes. In general, the proposed method may be applicable for any shape of original and internal virtual elements or combination both of them but that will be out of scope from this work. Second, similar to common computation with finite element method (FEM) a coordinate transformation between internal element and global original linear element coordinate must be determined before we proceed to finite element kinematics formulation. This transformation is relied on parametric representation of shape function. Linear tetrahedral kinematic formulation is used throughout this work including implementation of the VMR method. Since the formulation is very well known (e.g. [1]) and to focus more to our proposed method, it will not be described in this work.

According to [7], an example of deformation due to internal elements inside the original linear tetrahedral can be shown in Fig. 1. To accommodate for such behaviors we use tetrahedron volume meshed with auto meshing engine from GMSH [8] which is then simulated by using simple in-house FEM program. From the figure, we can simply consider the tetrahedron as a tetrahedral element located somewhere in a global meshed domain. Deformation shape is much improved by using large number of element (see Fig. 1d) which can be represented by continuous function, e.g. bubble function and enhanced strain. Here, instead of using the continuous function, we are relied directly with the result in Fig. 1 to minimize the artificial stiffness of the original tetrahedral element (here as Fig. 1a).

https://doi.org/10.1017/jmech.2016.113 Published online by Cambridge University Press

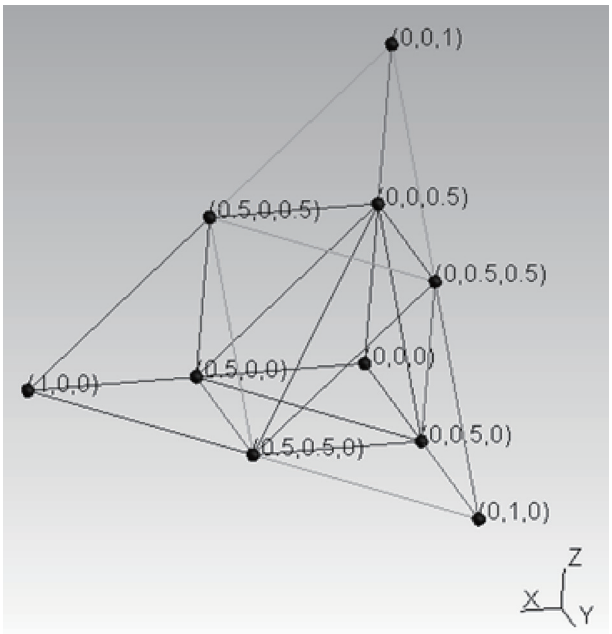


Fig. 2 Eight internal virtual tetrahedral elements with their corresponding nodes and parametric coordinate.

Instead of using auto meshing, we use more regular configuration as shown in Fig. 2 to form internal structure of virtual elements. Each node for each virtual element has a local parametric coordinate (ϕ, ϑ, η) with $0 < \phi < 1$, $0 < \vartheta < 1$ and $0 < \eta < 1$. To obtain its corresponding global coordinate $\vec{\mathbf{x}}_{\text{int}}$, the relation in (1) is applied.

$$\vec{\mathbf{x}}_{\text{int}} = \phi\vec{\mathbf{x}}_1 + \vartheta\vec{\mathbf{x}}_2 + \eta\vec{\mathbf{x}}_3 + (1-\phi-\vartheta-\eta)\vec{\mathbf{x}}_4 \tag{1}$$

The $\vec{\mathbf{x}}_1$, $\vec{\mathbf{x}}_2$, $\vec{\mathbf{x}}_3$ and $\vec{\mathbf{x}}_4$ are global coordinate of the internal nodes which are coincide with nodes from the original element, i.e. vertices in Fig. 2 with parametric coordinate (0, 0, 0), (1, 0, 0), (0, 1, 0) and (0, 0, 1). These nodes will be numbered specifically by 1, 2, 3 and 4.

After global coordinate of internal nodes are known, we can modify stiffness matrix of the original element by additional degree of freedom from the internal virtual element. According to Fig. 2, we can run an assembly process involving the 8 elements to form a new stiffness matrix represent a new distinct element. To label this new element, we will call it as "VMR element" henceforth. Shortly, the stiffness of the VMR element has the following form

$$\begin{bmatrix} \mathbf{K}_{11} & \mathbf{K}_{12} \\ \mathbf{K}_{12}^T & \mathbf{K}_{22} \end{bmatrix} \begin{bmatrix} \vec{\mathbf{u}}_1^{\text{int}} \\ \vec{\mathbf{u}}_2^{\text{int}} \end{bmatrix} = \begin{bmatrix} \vec{\mathbf{f}}_{ext} \\ \vec{\mathbf{0}} \end{bmatrix} \tag{2}$$

with

$$\vec{\mathbf{u}}_1^{\text{int}} = \begin{bmatrix} \vec{\mathbf{u}}_{1,1}^{\text{int}} & \vec{\mathbf{u}}_{1,2}^{\text{int}} & \vec{\mathbf{u}}_{1,3}^{\text{int}} & \vec{\mathbf{u}}_{1,4}^{\text{int}} \end{bmatrix}^T \tag{3}$$

as displacement for the nodes number 1-4 and

$$\vec{\mathbf{u}}_2^{\text{int}} = \begin{bmatrix} \vec{\mathbf{u}}_{2,5}^{\text{int}} & \vec{\mathbf{u}}_{2,6}^{\text{int}} & \dots & \vec{\mathbf{u}}_{1,i}^{\text{int}} \end{bmatrix}^T \tag{4}$$

as for the remaining internal node i.

Solving (2) for $\vec{\mathbf{u}}_1^{\text{int}}$ can be done by help of the 2nd row as follows

$$\vec{\mathbf{u}}_2^{\text{int}} = -\mathbf{K}_{22}^{-1}\mathbf{K}_{12}^T\vec{\mathbf{u}}_1^{\text{int}} \tag{5}$$

Inserting this to the 1st row in (2) we have

$$\mathbf{K}_{VMR}\vec{\mathbf{u}}_1^{\text{int}} = \vec{\mathbf{f}}_{ext} \tag{6}$$

with $\mathbf{K}_{VMR} = \mathbf{K}_{11} - \mathbf{K}_{12}\mathbf{K}_{22}^{-1}\mathbf{K}_{12}^T$. If it is compared to the static condensation proposed in general three field-formulation, e.g. in [3], Eq. 6 has similar in the form with additional internal deformation compatibility inter-element only across nodes not through element edges or faces. Moreover, this element stiffness $\mathbf{K}_{VMR}$ is then used for assembly process for global stiffness matrix replacing the original element.

Important remark is given here that we cannot directly consider stiffness in (6) for global assembly because with respect to the 4 main nodes it gives stiffer response than the original element. The reason for that is redistribution of displacement field which is now related not only to the main 4 nodes but also distributed over other internal nodes. However, in terms of energy produced for the same external load the stiffness $\mathbf{K}_{VMR}$ is larger than the stiffness from the original element due to more DOF involved. This fact gives us good opportunity to use the strain energy measurement as the starting point to minimize artificial stiffness of the original linear element.

2.2 Strain Energy and Stiffness

In FEM, we can measure strain energy in two ways. First, we return to the basic work conjugate relationship between stress and strain. And second, it is directly computed from stiffness matrix with the help of displacement measured. We use the latter because computation of stress and strain in the VMR element need to be re-defined. We leave it for future research and focus more in this work to minimize artificial stiffness with the help of energy from the original linear and the VMR element.

Using the same analogy to produce energy in one dimensional spring, we project $\mathbf{K}_{VMR}$ twice with respect to unknown displacement vector $\vec{\mathbf{u}}_1^{\text{int}}$ above as follows

$$W_{VMR} = \frac{1}{2}\left(\vec{\mathbf{u}}_1^{\text{int}}\right)^T \cdot \mathbf{K}_{VMR}\vec{\mathbf{u}}_1^{\text{int}}. \tag{7}$$

Here, we need initial value of $\vec{\mathbf{u}}_1^{\text{int}}$ which can be obtain only by running FEM simulation first using the original element and obtain some particular values for $\vec{\mathbf{u}}_1^{\text{int}}$. In this case, for each VMR element the energy in (7) is always related to actual deformation due to particular boundary condition applied. This is an ideal situation but in large scaled problem involving large number of tetrahedral element this approach is not efficient.

Instead, we use (7) with prescribing a displacement

https://doi.org/10.1017/jmech.2016.113 Published online by Cambridge University Press

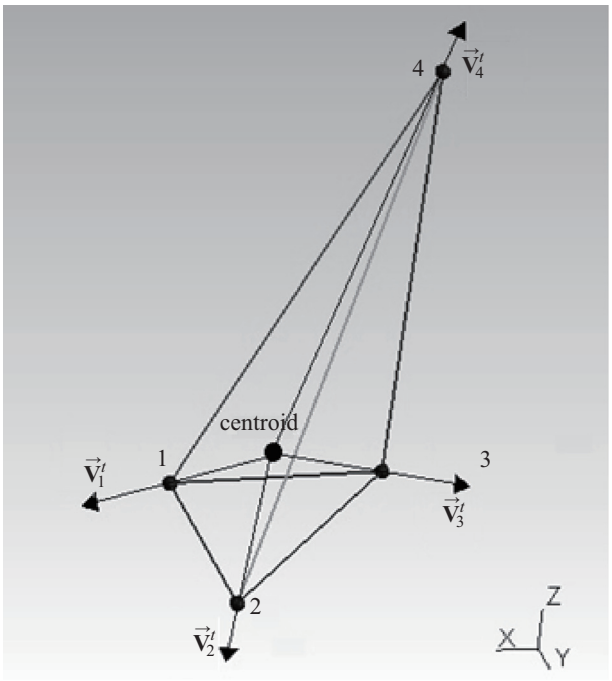


Fig. 3 Displacement test vectors $\vec{\mathbf{v}}_m^t$ for each main node number m direction with respect to tetrahedral centroid.

test vector $\vec{\mathbf{v}}_m^t$ which is arbitrary in nature and has ideal situation at $\vec{\mathbf{v}}_m^t = \vec{\mathbf{u}}_1^{\text{int}}$ with m as each 4 main nodes mentioned before. For qualitatively assessment of our proposed method only, we use a simple scenario with $\vec{\mathbf{v}}_i^t$ aligned with vectors connecting centroid of tetrahedral

$$\vec{\mathbf{x}}_c^{\text{int}} = \left(\vec{\mathbf{x}}_1 + \vec{\mathbf{x}}_2 + \vec{\mathbf{x}}_3 + \vec{\mathbf{x}}_4\right)/4 \tag{8}$$

to their 4 main nodes as shown in Fig. 3. It is obvious that there is significant difference in responses of the element in Fig. 3 with and without internal virtual elements. After the centroid of tetrahedral is obtained, we are ready to compute $\vec{\mathbf{v}}_m^t$ in normalized form as

$$\vec{\mathbf{v}}_m^t = \frac{\vec{\mathbf{x}}_m - \vec{\mathbf{x}}_c^{\text{int}}}{\left|\vec{\mathbf{x}}_m - \vec{\mathbf{x}}_c^{\text{int}}\right|} \tag{9}$$

for each nodes belonging to the original and VMR element . Consequently, the resultant of displacement vector $\vec{\mathbf{v}}_m^t$ does not generate torsional load with respect to centroid of tetrahedral but it causes tension-compression load to the element.

Finally, we are ready to obtain reduction factor to minimize artificial stiffness from the original tetrahedral element stiffness of $\mathbf{K}_{ORI}$, namely

$$R^W = \frac{(\vec{\mathbf{v}}_m^t)^T \cdot \mathbf{K}_{VMR}\vec{\mathbf{v}}_m^t}{(\vec{\mathbf{v}}_m^t)^T \cdot \mathbf{K}_{ORI}\vec{\mathbf{v}}_m^t}. \tag{10}$$

In order to contain the same energy amount due to $\vec{\mathbf{v}}_m^t$, we can simply modify $\mathbf{K}_{ORI}$ as

$$\mathbf{K}_{ORI}^* = R^W \mathbf{K}_{ORI}. \tag{11}$$

Remark for Eq. (11), it represents modification of energy independent with respect to particular direction of external applied loading in FEM modeling and simulation. Roughly speaking, we assume that both element will response exactly the same with respect to the same external loading. Another assumption comes from the use of the displacement test function $\vec{\mathbf{v}}_m^t$ which represents only specific loading condition. In this case, R^W only depends on geometry or shape of the VMR element, e.g aspect ratio of tetrahedral. Thus, for further improvement we may consider orientation of $\vec{\mathbf{v}}_m^t$ with respect to loading direction.

3. NUMERICAL EXAMPLES

In order to qualitatively show the potential use of the VMR element, we present 3 numerical examples starting from the most basic geometry of single tetrahedral until thin a shell problem. Although it is strongly not recommended in practice to deal with tetrahedral element meshing for shell structure, we show that even in such case the VMR element can improvement displacement field significantly with all above assumptions.

We repeat here the simulation in Fig. 1 but directly using one VMR element. It means that all internal elements appeared in Fig. 1 now become virtual with their new stiffness represented by Eq. 2 above. The VMR element is provided with 8 internal virtual elements exactly under the same boundary condition depicted in Fig. 1 with dimensionless external loading $\vec{\mathbf{f}}_{ext} = 10^3\left[1.5 \quad 1.5 \quad 1.5\right]^T$ N. Linear isotropic material model is used where bulk and shear modulus are related to the Young Modulus $E = 2.10^5$ MPa and poisson ratio $v = 0.3$ by

$$\mu = \frac{E}{2(1+\upsilon)} \tag{12}$$

$$\kappa = \frac{E}{3(1-2\upsilon)} \tag{13}$$

During simulation the influence of tetrahedral shape to amount of R^W is measured using metric γ (see [9]) by comparing its root-mean-square edge length to volume V as

$$\gamma = \frac{\sqrt{2}d_{rms}^3}{12\,V} \tag{14}$$

with $d_{rms} = \sqrt{\frac{6}{l=1}\sum S_l^2}$. The length S_l is evaluated for each l^{th} edge of the tetrahedral. The acceptable values of γ for an ideal tetrahedral is $1 < \gamma < 3$ (see Fig. 4 for some examples). The result shown in Fig. 5 clearly

https://doi.org/10.1017/jmech.2016.113 Published online by Cambridge University Press

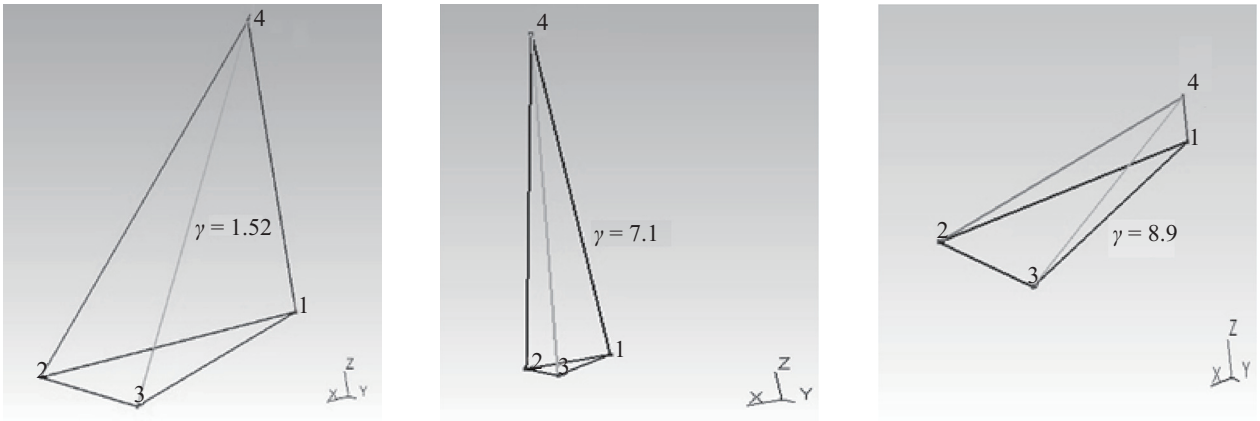


Fig. 4 Three different shape of linear elements from left to right with γ equal to 1.52, 7.1 and 8.9. It is obvious from this figure that they are distinct by distance between 1st and 4th node.

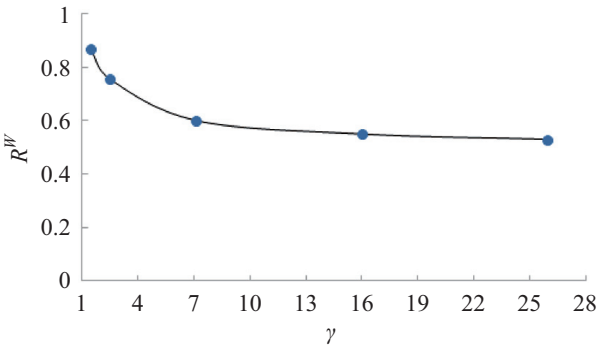
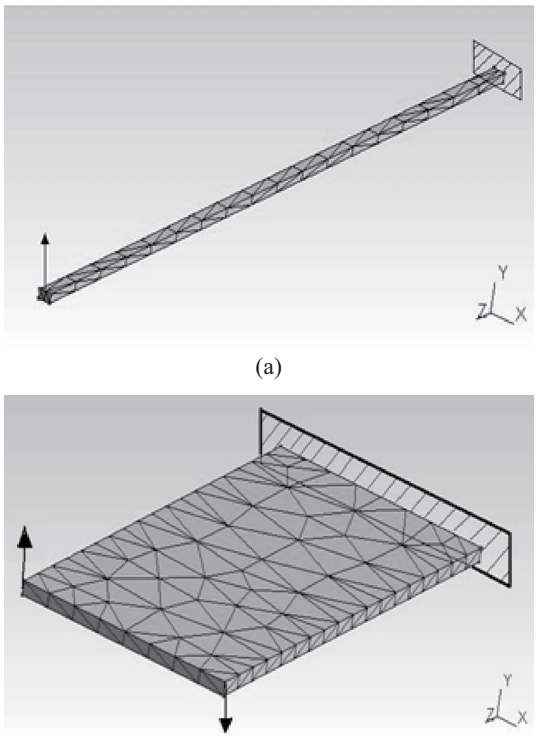


Fig. 5 Plot of R^W versus γ.



(a)

(b)

Fig. 6 Finite element mesh for numerical experiment for (a) cantilever beam and (b) thin shell with torsional loading (b). Both of them are fixed at the opposite of loading sides (shown by arrows).

indication that softening behavior increase if the shape of tetrahedral is out of ideal tetrahedral interval. However, after some value of γ it starts to almost constant.

Furthermore, we present two extreme cases of using tetrahedral element for very slender and thin structures. For the first case, the cantilever beam having rectangular cross section with b = 0.15 m, t = 0.1 m and length L = 10 m is loaded by F = 4408.9 N forces at its tip perpendicular to the length. We use the same material properties as previous single tetrahedral simulation. Under not sufficient fined meshing, this very slender cantilever contains much distorted tetrahedral element shapes and promotes strong artificial stiffness. Finer mesh with large number of tetrahedral element can reduce the locking but increase computational time. We will validate the potential used of the VMR element to reduce the artificial stiffness using relatively coarse mesh as shown in Fig. 6(a) with $\gamma > 3$ for most elements. Second case, a thin shell with length of 2 mm, width of 1 mm and 0.05 mm thickness is loaded with 10 N force acting coupled to form pure torsion. Material used here is again same with two previous case above.

The simulation results from both cases are shown in Figs. 7 and 8. Improvement for the cantilever tip deformation u_T almost 75% is obtained from the first simulation by using the VMR element compared to the original one. Although the improvement is quite significant, it is still far from the analytical solution

$$u_T = \frac{FL^3}{3Ebt^3} \tag{15}$$

which produce the tip displacement 588 mm or 4728% larger than using the VMR method. This huge deviation is promoted by very high artificial stiffness due to very slender tetrahedral used in the simulation. By measuring γ and typical trend shown in Fig. 5, further improvement can only be made by refine mesh to get better shape of tetrahedral element used. It means reduction of R^W but additional DOF in the cantilever is

https://doi.org/10.1017/jmech.2016.113 Published online by Cambridge University Press

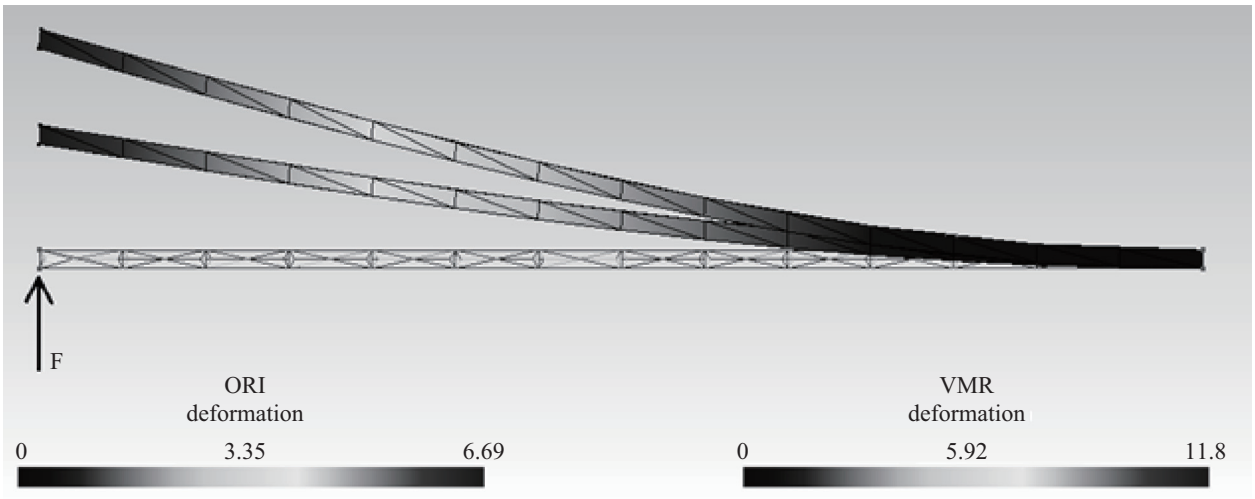


Fig. 7 Result from the original element versus the VMR element (VMR) for cantilever simulation.

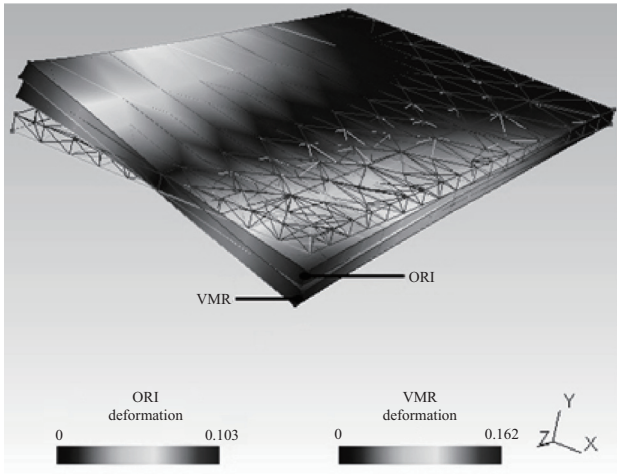


Fig. 8 Result from the original element (ORI) versus the VMR element (VMR) for thin shell torsion.

increase. On the other hand, by using the VMR element displacement in the shell simulation is also improved by order of 57% from the original element result. Here, the same consideration regarding γ in the cantilever simulation is applied as well.

Wang *et al.* [10] show that the potential improvement of the maximum stress for a cantilever meshed with tetrahedral elements is approximately 500% by using the quadratic tetrahedral element compared to the original one for the same number of element. This means that the tip displacement is also improved by approximately the same order by considering the analytical solution in (15). With only approximately 75% improvement using the VMR element means that there is still plenty of room for further improvement by using the VMR element. As we discuss in the Section 2, the capability of the VMR element in this work is limited by the displacement test vectors shown in Fig. 3 which omits torsional loads. The test vectors are not suitable for the cantilever problem where the main source of deformation is due to shear deformation modes normally induced by torsional loading cases. Hence, we need to find better test function for the next development stages which can represent not only tensile-compression but also shear dominated problems.

Moreover, although to the best of our knowledge the application of tetrahedral element for thin shell problem does not exist, we propose to solve such problem to represent a typical of extreme condition test for solid element. Many customized shell or shell-solid element have been developed for this case because the use of solid element is not practical due to huge number of element required to avoid very slender element shape with high artificial stiffness. Thus, we mean only to show that even in such worst case our proposed model can still work by reducing the artificial stiffness of very slender tetrahedral shape. Since the torsional loading is applied here, the same limitation from the use of the test vectors in Fig. 3 appears as well.

4. CONCLUSIONS

In small strain FEM simulation, the VMR method has succesfully minimize artificial stiffness of the 4-nodes linear tetrahedral by reducing its artificial stiffness. It is relied on additional DOF applied in the linear element due to internal virtual element. By using special displacement test vectors, the reduction is achieved by strain energy comparison between elements with and without the VMR method, i.e. the VMR element and the original or linear element, respectively. Due to the choice of the test vectors, shape of tetrahedral shows strong influence to the amount of reduction. Meanwhile, the simulation using the VMR element give improvement in displacement within range of 57% for cantilever to 75% in the shell with torsional loading simulation compared to the linear element. However, the improvement due to the VMR element in the cantilever simulation is insignificant compared to the corresponding analytical solution which is 4728% larger. It means that there is still plenty of room for improvement in the future.

https://doi.org/10.1017/jmech.2016.113 Published online by Cambridge University Press

ACKNOWLEDGEMENTS

I would like to thank for the financial support from Lembaga Pengelola Dana Pendidikan (LPDP) – RI through the Beasiswa Pendidikan Indonesia (BPI) and University of Jenderal Soedirman (UNSOED), Indonesia.

REFERENCES

1. Zienkiewicz, O. C. and Taylor, R. L., *The Finite Element Method*, Volume 1: The Basis. Butterworth-Heinemann, Oxford (2000).
2. Saucedo-Mora, L. and Marrow, T. J., "Method for the explicit insertion of microstructure in Cellular Automata Finite Element (CAFE) models based on an irregular tetrahedral Finite Element mesh: Application in a multi-scale Finite Element Microstructure MEshfree framework (FEMME)," *Finite Elements in Analysis and Design*, **105**, pp. 56-62 (2015).
3. Taylor, R. L., "A mixed-enhanced formulation for tetrahedral finite elements," *International Journal for Numerical Methods in Engineering*, **47**, pp. 205-227 (2000).
4. Thoutireddy, P., Molinari, J. F., Repetto, E. A. and Ortiz, M., "Tetrahedral composite finite elements," *International Journal for Numerical Methods in Engineering*, **53**, pp. 1337-1351 (2002).
5. Onishi, Y. and Ayama, K., "A locking-free smoothed finite element formulation (modified selective FS/NS-FEM-T4) with tetrahedral mesh rezoning for large deformation problems," *The 11th World Congress on Computational Mechanics (WCCM XI)*, Barcelona, Spain (2014).
6. Ostien, J. T., Foulk, J. W., Mota, A. and Veilleux, M. G., "A 10-Node Composite Tetrahedral Finite Element for Solid Mechanics," *International Journal for Numerical Methods in Engineering*, 10.1002/nme.5218 (2016).
7. Waluyo, S., "Accuracy improvement for linear tetrahedral finite element by means of virtual mesh refinement," *Journal of Mechanical Engineering, University Technology Mara*, **12**, pp. 19-30 (2015).
8. Geuzaine, C. and Remacle, J. F., "Gmsh: a three dimensional finite element generator with built-in pre- and post-processing facilities," *International Journal for Numerical Methods in Engineering*, **79**, pp. 1309-1331 (2009).
9. Parthasarathy, V. N., Graichen, C. M. and Hathaway, A. F., "A comparison of tetrahedron quality measures," *Finite Elements in Analysis and Design*, **15**, pp. 255-261 (1994).
10. Wang, E., Nelson, T. and Rauch, R., "Back to elements-tetrahedra vs. hexahedra," *Proceedings of the 2004 International ANSYS Conference* (2004).

(Manuscript received July 23, 2016,
accepted for publication October 21, 2016.)

https://doi.org/10.1017/jmech.2016.113 Published online by Cambridge University Press